Theoretical Studies of the Reductive C−S Bond Cleavage in Complexes of the Form $[M(9S3)_2]^{2+}$ (M = Re, Tc, and Ru; 9S3 = 1,4,7-Trithiacyclononane)

Patrick Maurer,[†] Alessandra Magistrato,[‡] and Ursula Rothlisberger[†,*]

Laboratory of Inorganic Chemistry, Federal Institute of Technology ETHZ, ETH Hönggerberg, CH-8093 Zürich, Switzerland

Received: September 27, 2004

We have applied Density Functional Theory (DFT) at the generalized gradient approximation (GGA) level to investigate the C−S bond cleavage in hexathioether complexes of the form $[M(9S3)_2]^{n+}$ (with 9S3 = 1,4,7-trithiacyclononane and M = Re, Tc; n = 1, 2; as well as M = Ru; n = 2, 3). The experimental trends in C−S bond lengths of the different compounds[1] are reproduced faithfully. Reduction leads to a lowering of the calculated reaction energies by ≈20 kcal/mol to values of 4, 10, and 44 kcal/mol for M = Re, Tc, Ru, respectively. The corresponding values for the activation energy are 10, 15, and 44 kcal/mol, which is in agreement with the experimental observation that the rhenium and technetium compounds lose an ethene molecule immediately after reduction, while the ruthenium compound is stable toward such a loss. Our calculations suggest that the unique reactivity of the reduced rhenium and technetium complexes is a result of the higher energies of metal t_{2g}-orbitals, resulting from the lower overall charge of the complex. π-Back-donation from t_{2g}-orbitals into C−S σ*-orbitals is another important effect, leading to low activation barriers, as only little electronic rearrangement is necessary upon cleavage of the C−S bonds.

1. Introduction

Metal complexes containing the γ-emitting radio isotope technetium-99m are widely used in modern medicine as they enable the monitoring of biological functions and constitute convenient devices for the imaging of tissues, organs, and tumors.[2] The increased ability to target radiopharmaceuticals to specific locations in the body has opened the possibility of radiotherapeutic treatment of cancerous tissue with radiation that is generated in situ, by delivering a suitable radionuclide to the tumor,[3,4] instead of applying radiation from an external source.

The β-emitting rhenium isotopes ^{186}Re and ^{188}Re are particularly interesting for such applications, due to their excellent physical properties and availability and their chemical analogy with technetium.[5] Investigations of the chemistry of rhenium and technetium with the ligand 1,4,7-trithiacyclononane (9S3) have led to a new class of compounds $[M(9S3)_2]^{2+}$, which exhibit interesting redox properties:[5] when they are reduced electrochemically or treated with mild reducing agents such as ascorbate or metallic zinc, in aqueous solution and at room temperature, immediate cleavage of two C−S bonds is observed, leading to the formation of ethene and $[M(9S3)L]^+$ (M = Re, Tc; L = $[S(CH_2)_2S(CH_2)_2S]$).

Other hexathioether compounds of the form $[M(9S3)_2]^{n+}$, where M are metals from groups 7−12 of first, second, and third row transition metal elements and n = 1−3, have been synthesized and characterized,[6] but the C−S bond fission is only observed in the case of the rhenium and technetium compounds. However, a clear correlation exists between the mean C−S bond length of the coordinated thioether ligand and the position of M in the periodic table.[1] Within a given group the first row metal complexes present the shortest C−S bond lengths, while they increase with decreasing group number. These observations have been explained in terms of π-back-donation from donor t_{2g} metal orbitals into empty C−S σ*-orbitals,[1] a hypothesis that is supported by experimental studies[7] and semiempirical calculations at the Extended Hückel Theory (EHT) level[7] as well as first-principles MD studies based on density functional theory.[8]

Moreover, the degree of bond elongation in a given metal complex differs for the two C−S bonds of each thioether unit, due to the fact that only one of them lies in the plane of a filled metal t_{2g}-orbital[1] and thus the overlap of the C−S σ*-orbital with the metal donor orbital is more efficient compared to the "out-of-plane" C−S bond. Again, this effect is more pronounced in complexes with transition metals on the left of the periodic table.[1]

On the basis of this π-back-donation model, the observed release of ethene from the technetium and rhenium compounds upon reduction of the d^5 complexes to their d^6 analogues simply represents the extreme of a trend,[5,7] as C−S bond activation becomes sufficient to induce a complete cleavage of the bond upon reduction.

The ease with which C−S bond cleavage can be induced in these compounds suggests them as homogeneous model systems for the complex processes involved in hydrodesulfurization (HDS). HDS is a heterogeneously catalyzed, large-scale industrial process during the refinement of crude oils in order to reduce the sulfur content. Obviously, this reaction is of great practical importance, and it may become even more so due to stricter environmental regulations on sulfur content in gasoline and other fuels.

We have recently performed a detailed ab initio molecular dynamics study of the mechanism of ethene dissociation from $[Re(9S3)_2]^{n+}$ (n = 1, 2),[8] which showed that the fission of the

* To whom correspondence should be addressed: ursula.roethlisberger@epfl.ch.

[†] Current address: Institute of Molecular and Biological Chemistry, Federal Institute of Technology EPFL, CH-1015, Lausanne, Switzerland.

[‡] Current address: INFM-Democritos Center and International School of Advanced Studies (SISSA/ISAS), Via Beirut 2-4, I-34014 Trieste, Italy.

10.1021/jp045615n CCC: $27.50
Published on Web 12/04/2004

two C−S bonds occurs quasi simultaneously as a separate reaction step after reduction of the complex, with a calculated activation energy of 10 kcal/mol.

In the present work, we have compared the above rhenium d^5- and d^6-complexes to their technetium analogues, which exhibit similar reactivity, as well as to their ruthenium analogues, which are stable toward the loss of ethene. In particular, we have investigated similarities and differences in their redox and catalytic behavior in order to rationalize experimental observations. We have performed a detailed characterization of the structural and electronic properties of these complexes using density functional theory (DFT) methods at the generalized gradient approximation (GGA) level. Dissociation and activation energies for ethene dissociation are reported and compared to experimental findings.

The C−S bond cleavage reaction also represents an excellent test case for our computational approach in view of its application to more complex radiopharmaceutical compounds.

2. Details of the Computational Scheme

Static and dynamic[9−11] calculations have been carried out with the program CPMD,[12] which is an implementation of the original Car−Parrinello scheme based on density functional theory, periodic boundary conditions, plane wave basis sets, and a pseudopotential approach.

In this work, we used an analytic local pseudopotential for hydrogen atoms and nonlocal, norm-conserving soft pseudopotentials of the Martins−Trouiller type[13] for all other elements. Angular momentum components were included up to $l_{max} = 1$ for carbon and $l_{max} = 2$ for sulfur. For rhenium we used the same pseudopotential as in our previous work.[8] For technetium and ruthenium we have constructed semicore pseudopotentials with ionic reference states of $4s^24p^64d^65s^0$ and $4s^24p^64d^75s^0$, respectively. Cutoff radii are $r_s = 0.92$ au, $r_p = 1.1$ au, $r_d = 1.35$ au for technetium and $r_s = 1.2$ au, $r_p = 1.2$ au, $r_d = 1.4$ au for ruthenium. All valence electrons (13 for d^5 ions and 14 for d^6 ions, respectively) have been treated explicitly and the pseudopotentials for the three metals incorporate scalar relativistic effects. The pseudopotentials for carbon and sulfur were transformed to a fully nonlocal form using the scheme of Kleinman and Bylander,[14] whereas for all the transition metals the nonlocal part of the pseudopotentials was integrated numerically using a Gauss−Hermite quadrature.

Since the quality of these transition metal pseudopotentials is crucial to our computational approach, we performed test calculations on small molecules for which structural information from electron diffraction experiments or other theoretical data are available, namely TcO_2F_3[15] and RuO_4.[16] Bond lengths in both molecules are reproduced within $\Delta d \leq 0.01$ Å, with the exception of the Tc−O bonds in TcO_2F_3, where the agreement is within $\Delta d \leq 0.02$ Å.

Two different gradient-corrected exchange-correlation energy functionals were used. The exchange part was in both cases described by the functional developed by Becke,[17] whereas for the description of the correlation part we used either the functional of Perdew[18] or the one by Lee, Yang, and Parr.[19] The resulting widely used exchange-correlation energy functionals are usually referred to as BP and BLYP, respectively.

Molecular structures were optimized using a preconditioned conjugate gradient algorithm as implemented in the program CPMD. For the molecular dynamics runs, the classical equations of motion were integrated with a velocity Verlet algorithm with a time step of 0.145 fs and a ficticious mass for the electronic degrees of freedom of $\mu = 400$ au. All calculations were carried out in a simple cubic cell with a boxlength $l = 25$ au, with a kinetic energy cutoff of 70 Ry for the plane wave basis set, in a spin unrestricted formalism. Charged periodic images were decoupled using the scheme of Hockney.[20]

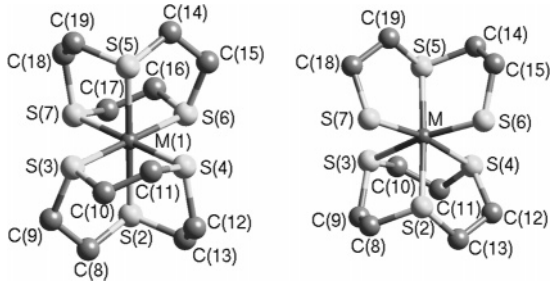

Figure 1. Structures of the reactant (left) and product (right) compounds with the numbering scheme used throughout this work. Shown are the calculated structures with $M = Ru^{2+}$. Hydrogen atoms are omitted for clarity.

3. Results and Discussion

3.1. Structural Properties. A schematic representation of the reactant and product compounds together with the numbering scheme used throughout this work is given in Figure 1.

In a first step, we compare structures optimized with both exchange-correlation functionals (BP and BLYP) with crystallographic data. For the reactants $[M(9S3)_2]^{2+}$ such data is available for M = Re,[21] Tc,[22] and Ru,[23] whereas for the product $[M(9S3)L]^+$ crystallographic information is only available for M = Re[1] and Tc.[5] As a starting point for our calculations of the reactants, we chose the crystal structure of $[Re(9S3)_2]^{2+}$ for all metal centers. For the ruthenium compound an additional calculation was performed starting from the crystal structure of $[Ru(9S3)_2]^{2+}$. Both calculations of the ruthenium complex yield the same optimized geometry (root-mean-square deviation (RMSD) $\approx$ 0.0003 Å/atom), indicating that to a great extent the optimized geometries do not depend on the initial atomic coordinates. In an analogous manner, we chose the X-ray structure of $[Re(9S3)L]^+$ as the starting point for optimizing the structures in the product state. Selected bond lengths of calculated and available X-ray structures of reactant and product compounds are presented in Table S1. For the sake of comparison, we also include the results from our previous calculations[8] with M = Re.

For the reactants, the agreement between calculated and X-ray structures is excellent for all three metal centers (RMSD $\approx$ 0.01 Å/atom). The BP functional leads to better agreement with experiment than the BLYP functional, in agreement with our previous study[8] on $[Re(9S3)_2]^{2+}$ and other studies on transition metal complexes.[24,25] All bond lengths in all three reactant compounds are reproduced within $\Delta d \leq 0.03$ Å with the BP functional, while BLYP yields consistently longer bond lengths with an agreement within $\Delta d \leq 0.06$ Å. The small difference ($\approx$0.02 Å) between "in-plane" and "out-of-plane" C−S bonds is reproduced faithfully in all calculations.

In the product compounds $[Re(9S3)L]^+$ and $[Tc(9S3)L]^+$, the deviation with respect to experimental structures is slightly larger. Bond lengths are reproduced within $\Delta d \leq 0.05$ Å in both compounds, with the exception of the two bonds M−S(3) and M−S(4), which are in trans position to the thiolate ligands. For these two bonds we observe deviations from the experimental values in a range of 0.01 Å (BP, M = Tc) to 0.14 Å (BLYP, M = Re).

For the same two bonds we also observe the largest change in bond length of $\Delta d \approx 0.06$ Å upon changing the exchange-

correlation functional from BP to BLYP, compared to a change in all other bonds of $\Delta d \leq 0.04$ Å. This difference indicates that the product compounds are more sensitive to the description of electron correlation than the reactants, especially concerning the description of the two metal-sulfur bonds in axial position to the thiolate sulfur atoms S(6) and S(7).

The overall excellent agreement between crystallographic and calculated structures shows that our computational approach is adequate for the description of these compounds. It is also an indication that the pseudopotentials for the transition metals are of comparable quality for complexes in which a high valent metal center is coordinated by "hard" ligands such as oxide or fluoride (e.g. TcO_2F_3 or RuO_4, see Section 2) and for compounds containing low valent metal centers and ligands with "soft" donor atoms, such as sulfur.

As a second part of this study, we examined the influence of the oxidation state of the metal center on structural properties of both the reactant and the product compounds. For this purpose, we optimized the structures of the reactants and products with both d^5 and d^6 ions of technetium and ruthenium as the reactant metal center, i.e., $[Tc(9S3)_2]^{n+}$, $[Tc(9S3)L]^{n+}$ ($n = 1, 2$) and $[Ru(9S3)_2]^{n+}$, $[Ru(9S3)L]^{n+}$ ($n = 2, 3$). Selected structural parameters of all the calculated structures are given in Table S1. Again, we include the results from our previous study[8] with M = Re and $n = 1, 2$ for comparison.

Our calculations show that all six compounds correspond to local minima on the potential energy surface, which implies that the dissociation of ethene does not take place simultaneously with the reduction of the metal center, but occurs as a subsequent reaction step. We have previously performed a detailed ab initio molecular dynamics study of the dissociation of ethene from $[Re(9S3)_2]^+$,[8] which shows that the additional electron lowers the reaction barrier to such an extent that the dissociation of an ethene molecule can be observed within 4 ps simulation time at 350 K.

In the reactants the structural changes upon reduction of the metal centers are small. There is a general shortening of the M−S bonds by ≈0.02 Å for rhenium and ruthenium and by ≈0.03 Å for technetium, indicating a slightly stronger bond which can be attributed to a preference of sulfur donor atoms to coordinate metal ions in low oxidation states, with increasing covalent interactions. The C−S bond lengths in the ruthenium complex are not significantly influenced by the additional electron, whereas in the other two compounds we observe an elongation by ≈0.02 Å (M = Tc) and ≈0.04 Å (M = Re), respectively. These findings parallel the trends in the calculated bond orders[27] (BO), which are given in Table S2 for both the reactant and product compounds. In $[Ru(9S3)_2]^{3+}$, a slight increase of $\Delta BO = 0.01$ for the Ru−S bonds is calculated upon reduction, while the C−S bond orders remain unchanged. As a contrast, in $[Tc(9S3)_2]^{2+}$, we do not only find an increase of $\Delta BO = 0.02$ for the Tc−S bond orders, but also a decrease in all "in-plane" C−S bond orders of $\Delta BO = 0.03$ and of $\Delta BO = 0.02$ in all "out-of-plane" C−S bonds after the addition of an electron. This effect is still more pronounced in $[Re(9S3)_2]^{2+}$ with an increase of $\Delta BO = 0.03$ for the Re−S bonds and a decrease of $\Delta BO = 0.03$ for all C−S bonds.

In Figure 2, the calculated C−S bond lengths (BP functional) in the d^6 and d^5 reactant complexes of rhenium, technetium, and ruthenium as well as in the free ligand 9S3 are depicted graphically. All C−S bonds in the metal complexes are elongated compared to the free ligand. The changes in bond lengths and bond orders upon reduction are certainly consistent with enhanced π-back-donation. Given the completely different

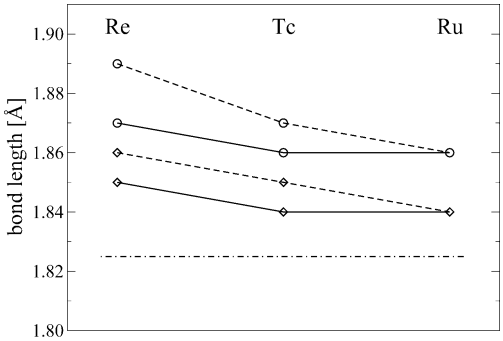

Figure 2. Calculated C−S bond lengths (Å) in the reactants (BP functional). Circles indicate "in-plane" C−S bonds, and diamonds indicate "out-of-plane" C−S bonds. Solid lines indicate a d^5 metal center, and dotted lines indicate a d^6 metal center. The dashed horizontal line indicates the mean C−S bond length in the free ligand 9S3 (BP functional).

TABLE 1: Adiabatic Electron Affinities EA (kcal/mol) for Reactant and Product Compounds

	BP			BLYP		
	Re[8]	Tc	Ru	Re[8]	Tc	Ru
reactant	−204.3	−204.5	−314.4	−198.5	−198.3	−307.5
product	−222.5	−225.7	−334.9	−216.6	−220.4	−334.9
ΔEA[a]	−18.2	−18.1	−21.2	−22.1	−20.5	−20.9

[a] ΔEA is calculated as $\Delta EA = EA_{(product)} - EA_{(reactant)}$.

reactivity of the of the reduced compounds, the changes are however rather subtle, notably in the case of Tc.

As for the reactants, the influence of the additional electron on the structural properties of the products is small, with the exception of the bond M−S(4) in the rhenium and technetium complexes. As mentioned above, this bond is highly sensitive to the correlation energy functional. The fact that the calculated changes in the bond length upon reduction are not consistent suggests that the different description of electron correlation has a larger influence on the properties of this bond than the additional electron. In $[Re(9S3)L]^{2+}$ an elongation of this bond by $\Delta d = 0.1$ Å upon reduction is calculated with the BLYP functional, while the BP functional predicts an elongation by $\Delta d = 0.05$ Å. For the technetium complex, both functionals predict a shortening upon reduction, by $\Delta d = 0.02$ Å (BLYP) and by $\Delta d = 0.06$ Å (BP), respectively. All other metal−sulfur bond distances change by $\Delta d \leq 0.03$ Å for all three metals upon changing the functional. Again, the calculated bond orders shown in Table S2 are fully consistent with the changes in bond length.

3.2. Dissociation and Activation Energies. As a third part of this project, dissociation energies and corresponding activation energy barriers for the dissociation of ethene from the d^6 and d^5 complexes of technetium and ruthenium were calculated and compared to the values of the corresponding rhenium complexes.[8] In Table 1, the adiabatic electron affinities (EA) for product and reactant compounds, calculated as $EA = E_{(d^6)} - E_{(d^5)}$, are reported. The electron affinities calculated with the BLYP functional are consistently about 6 kcal/mol higher than the ones calculated with BP, the energetic ordering however is the same for both functionals and the difference in electron affinity (ΔEA) between the reactant and product compound agrees within <1 kcal/mol. The calculated values show that electron attachment is strongly exothermic (≈200 kcal/mol for rhenium and technetium and >300 kcal/mol for ruthenium) for all complexes. The large increase in the electron affinities of the ruthenium compounds with respect to the rhenium and

TABLE 2: Dissociation Energies ΔE and Activation Energies E_A (kcal/mol) for the Dissociation of Ethene from d^6 and d^5 Reactant Compounds

	BP			BLYP		
	Re^8	Tc	Ru	Re^8	Tc	Ru
$\Delta E(d^5)$	22	30	64	14	19	53
$\Delta E(d^6)$	4	10	44	−4	−3	32
$E_A(d^5)$	21[a]	−[b]	−	−	−	−
$E_A(d^6)$	10	15	−	8	7	−

[a] See ref 28. [b] A dash indicates that no transition state could be located and in these cases $E_A = \Delta E$.

technetium analogues can clearly be attributed to the differences in nuclear charge of the metal centers.

The stabilization upon reduction is ≈20 kcal/mol higher in the product compounds compared to the reactant ones. Since the four different species for a given metal center form a thermodynamic cycle, it follows that the reaction energy must be lowered by the same value upon reduction.

The larger EA of the product compounds can be attributed to the higher oxidation state of the metal center, as the dissociation of ethene involves an intramolecular redox reaction where the metal center donates two electrons to cleave the C−S bonds.

Dissociation energies ΔE are calculated as $\Delta E = E_{(product)} + E_{(ethene)} - E_{(reactant)}$. Activation energies were determined by defining an appropriate reaction coordinate and by performing constrained molecular dynamics runs along it. Like in our previous work,[8] two different reaction coordinates were used: In the first case, a dummy atom (D) was placed at the bond midpoint of the two carbon atoms of the dissociating ethene group and an M−D distance constraint was applied and varied in increments of $\Delta d = 0.1$ Å. In the second case, a simple bond constraint for one of the two C−S bonds of the thioether ligand was applied and varied in similar intervals. The transition states were located by the change of sign in the average constraint force.

It turns out that in the case of both rhenium and the reduced technetium compounds, the two reaction coordinates are equivalent. In the case of the Tc(d^5) compound we observed not only strong hysteresis effects, but also a clear dependence on the choice of the constraint coordinate in regions close to a putative transition state, with energies differing by a few kcal/mol. A third reaction coordinate was therefore defined in this region by placing one dummy atom again at the C−C bond midpoint of the ethene moiety and a second dummy atom at the midpoint between the two adjacent sulfur atoms S(6) and S(7). The distance constraint was then applied to the distance of the two dummy atoms. Of all three reaction coordinates, the third one yielded the lowest energies and a barrierless potential energy curve which approaches the reaction energy asymptotically, i.e., a transition state could no longer be located. The transition state of the reduced Tc compound is highly similar to the one found for the Re analogue[8] and will not be discussed in detail here.

In the case of ruthenium, the first reaction coordinate (M−D distance) leads to an elongation of the two M−S bonds instead of the two C−S bonds, so that no dissociation of ethene occurs. This is a further indication of weaker M−S bonds (and/or stronger C−S bonds) in the ruthenium compounds compared to those of rhenium and technetium.

In Table 2, the calculated dissociation energies ΔE and activation energies E_A are presented. The dissociation from both ruthenium compounds is endothermic by >40 kcal/mol (BP functional), and no transition state could be located. Instead, the potential energy calculated with the BP functional approaches the dissociation energy asymptotically upon elongation of the C−S bonds. The BLYP functional predicts considerably lower (by ≈12 kcal/mol) reaction energies. With the BLYP functional we did not follow the entire reaction path, but optimized only one molecular structure, starting from the transition state of the rhenium d^6 compound while keeping the C−S bond length fixed ($d = 2.9$ Å). The energy of this structure lies 6 kcal/mol below the dissociation limit.

In the case of the Tc and Re complexes, reaction energies are significantly lower. In the d^5 compounds, the dissociation of ethene is endothermic by 22 kcal/mol (BP functional) and by 14 kcal/mol (BLYP) for rhenium and by 30 kcal/mol (BP) and 19 kcal/mol (BLYP) for technetium. As mentioned above, the additional electron lowers the reaction energy of the d^6 compounds by ≈20 kcal/mol. For the reduced rhenium and technetium compounds the BP functional predicts endothermic reactions, whereas BLYP in contrast predicts slightly exothermic reactions. The considerable differences in the reaction energies between the two exchange-correlation energy functionals can again be attributed to the strong sensitivity of the product compounds toward the description of electron correlation.[29] It should also be noted that the dissociation of ethene is an entropically favored process, which means that the values of the reaction free energy are expected to be lower than the calculated reaction energies.

An activation energy of $E_A = 21$ kcal/mol for $[Re(9S3)_2]^{2+}$ is calculated with the BP functional, whereas the additional electron in $[Re(9S3)_2]^+$ reduces this barrier to $E_A = 10$ kcal/mol. In the case of technetium the activation energy is lowered from 30 kcal/mol to 15 kcal/mol (BP). These values agree well with experiment in that ethene dissociation is only observed in the rhenium and technetium compounds and only after reduction to the d^6 complex,[1] whereas no ethene loss from $[Ru(9S3)_2]^{2+}$ was observed under solution conditions.[7] They are also in agreement with electrospray mass spectroscopy experiments,[7] where fragmentation and ethene loss in $[M(9S3)_2]^{2+}$ (M = Re, Tc, Ru, Os) was investigated. The reduced rhenium and technetium compounds readily loose an ethene molecule at low cone voltages, whereas for the ruthenium complex three times higher voltages are necessary for fragmentation to occur. The values are also in agreement with the observation that the Re^{2+} complex fragments more readily than the Tc^{2+} analogue.[7]

The reaction energies of the nonreactive compounds as well as the absence of an activation barrier clearly indicate that the chemical inertness toward loss of ethene is a thermodynamic rather than a kinetic effect. The reason for the high reaction energy can be rationalized upon investigation of the highest occupied molecular orbitals of the different species. A graphical representation of these orbitals is shown in Figures S1 and S2. HOMO to HOMO-2 of all reactant species correspond to metal t_{2g}-orbitals, while HOMO-3 and HOMO-4 can be identified as sulfur lone-pairs. In the product complexes of Re^+ and Tc^+ (which effectively contain an M^{3+} metal center), HOMO and HOMO-1 correspond to metal t_{2g}-orbitals, and HOMO-2 to HOMO-4 to sulfur lone-pairs. In the product complexes of Tc^{2+} and Ru^{2+}, on the other hand, the three highest MO show strong delocalization over the metal center and thiolate ligand atoms. This can be interpreted as partial charge transfer from the readily oxidizable thiolates to the metal center that formally is in the relatively high oxidation state IV.

The eigenvalues of the orbitals discussed above are shown in Figure 3 (for the product compounds, we show the eigenvalue of the HOMO of an isolated ethene molecule, i.e., the C−C π-orbital, instead of the HOMO-4 of the metal complex). It is

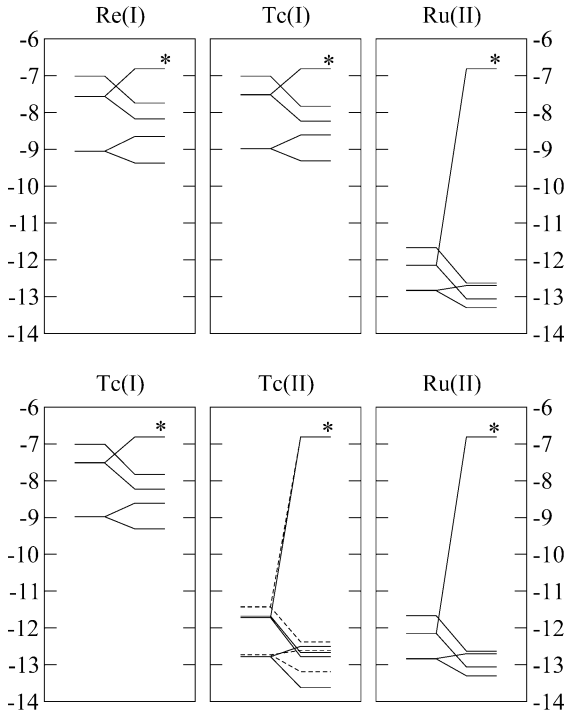

Figure 3. Eigenvalues (eV) of the five highest molecular orbitals, in the reactant (left side of each panel) and product state (right side of each panel). The corresponding orbitals are depicted graphically in Figures S1 and S2. The highest eigenvalue in the product states (indicated with a star) corresponds to the π-bond in an isolated ethene molecule. In the panel for the Tc(II) compounds, dashed and solid lines are used to distinguish electrons with α- and β-spin, respectively.

apparent from Figure 3 that the high reaction energy of the M^{2+} compounds is a result of the energy needed to promote two electrons from a metal t_{2g}-orbital into the π-bond of the departing ethene molecule. In the reduced reactants with an M^{+}-center and high lying t_{2g}-orbitals, on the other hand, the energy for promotion is substantially smaller, and is in fact more than compensated by the stabilization of the remaining t_{2g}-orbitals upon oxidation of the metal center. A positive contribution to the reaction energy however also stems from the higher eigenvalues of other orbitals in free ethene, compared to a C_2H_4 moiety in the 9S3 ligand (data not shown).

The above results lead to the conclusion that the main factor governing the reaction energy is the overall charge of the reactant. In fact, the changes on the electronic level are almost identical for the Tc^{2+} and the Ru^{2+} compounds (Figure 3), as are the calculated reaction energies of 30 and 32 kcal/mol, respectively (BP). The same observation holds for the Re^{+} and Tc^{+} compounds. The small difference in reaction energies must be attributed to subtle effects, the investigation of which is beyond the scope of this article. However, the slightly higher reaction energy of Tc^{+} is consistent with the well-known experimental trend that Tc compounds are generally harder to oxidize than their Re analogues.

The above considerations suggest that the π-back-donation effect discussed earlier is responsible for elongated C−S bonds, but has little consequences on the reactivity of the compounds, since the reaction energy is essentially governed by the overall charge. Furthermore, the structural changes upon reduction are small, and the characteristics of the chemically relevant orbitals remains largely unchanged (Figures S1 and S2, ref 8). A low reaction energy however is not sufficient for a reaction to occur spontaneously, as the reaction could still be prevented by a high activation barrier. Such a barrier could, for example, be caused by a substantial rearrangement of the electronic structure during the reaction. As discussed above, we do not find high activation barriers in the C−S bond cleavage reaction investigated here, and in this respect the π-back-donation appears to play an essential role.

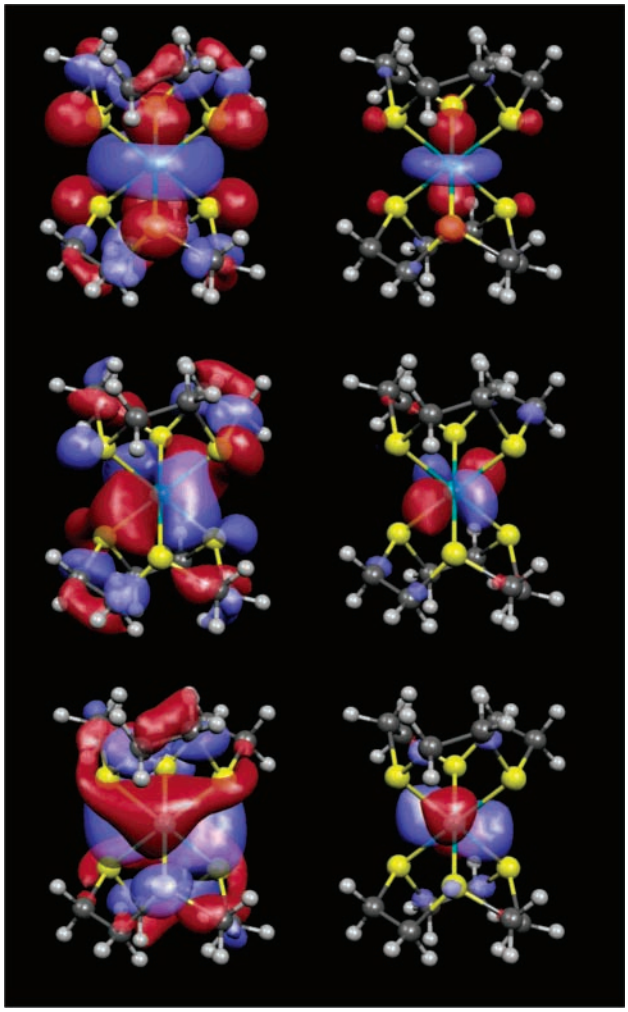

Figure 4. Contour plots of (from top to bottom) the HOMO, HOMO-1, and HOMO-2 of $[Tc(9S3)_2]^{+}$ showing π-back-donation from metal $d(t_{2g})$-orbitals into C−S σ*-ligand orbitals. Contours are shown at ± 0.02 au (left) and ± 0.05 au (right). Figure created with the programm Molekel.[26]

Figure 4 shows isocontour plots of the three highest molecular orbitals of $[Tc(9S3)_2]^{+}$. The contours drawn at ± 0.05 au (Figure 4, right) clearly identify these orbitals as metal t_{2g}-orbitals. The contours drawn at ± 0.02 au (Figure 4, left) confirm the π-back-donation into C−S σ*-orbitals and exhibit a significant amount of π-bonding on the ligand C−C bonds. This observation is confirmed by the calculated C−C bond orders of 1.5 (Table S2). Thus, there exists a partial "preformation" of C−C π-bonds in the reactant compounds, so that only small rearrangements in the electronic structure occur upon dissociation of an ethene molecule, which in turn leads to a low (or absent, in the case of reactants with charge 2+) activation barrier.

4. Conclusions

In this study, we compared the reductive C−S bond cleavage in complexes of the form $[M(9S3)_2]^{2+}$ (M = Re, Tc, Ru and 9S3 = 1,4,7-trithiacyclononane). We have performed a detailed structural and electronic characterization of reactant and product compounds with d^5 and d^6 metal centers by means of DFT at

the gradient corrected level. The agreement between calculated and X-ray structures is very good with a root-mean-square deviation (RMSD) of ≈0.01 Å/atom.

The influence of the additional electron upon reduction of the d^5 complexes to their d^6 analogues has also been investigated. Our calculations show that all d^6 complexes correspond to local minima on the potential energy surface and that the influence of the additional electron on structural properties in the ground state is only small. This implies that the immediate C−S bond cleavage upon reduction, which is observed in $[M(9S3)_2]^{2+}$ (M = Re, Tc)[1], occurs as a subsequent reaction step after the electron transfer. The observed difference in reactivity between d^6 and d^5 complexes is due to a lowering of the reaction energy by ≈20 kcal/mol upon reduction.

The calculated reaction energies are 4 kcal/mol and 22 kcal/mol for the d^6 and d^5 rhenium compounds, respectively, and 10 kcal/mol and 30 kcal/mol for technetium. These values are in agreement with the experimentally observed instability of the rhenium and technetium d^6 complexes[1]. In $[Ru(9S3)_2]^{2+}$, which is a d^6 complex but contains Ru(II) as opposed to Re(I) and Tc(I), an activation energy of 44 kcal/mol is calculated, in agreement with the experimental observation that under solution conditions no dissociation of ethene is observed from the ruthenium complex.[7]

Our results clearly support the model of π-back-donation from donor t_{2g}-metal-orbitals into antibonding σ^*-orbitals of ligand C−S bonds,[1] which leads to an elongation of C−S bonds compared to the free ligand. This π-back-donation is however a general feature of all complexes investigated here; reduction has a relatively small influence on this effect. The enhanced reactivity of the reduced compounds is caused not so much by a strong activation of the C−S bonds through the additional electron, but is rather a general effect of the lower overall charge and the associated higher eigenvalues of reactant molecular orbitals, so that less energy is needed to promote electrons from molecular orbitals of the reactant to those of the dissociating ethene. The π-back-donation into C−S σ^*-orbitals is however essential for the reactivity, as the small electronic rearrangement upon ethene dissociation leads to a low activation barrier.

With respect to HDS, our results imply a considerable catalytic potential for low valent complexes of Re and other elements to the left in the periodic table. The use of Tc as a catalyst is clearly ruled out by the fact that only radioactive isotopes exist.

Acknowledgment. We thank the Swiss Federal Institute of Technology Zurich and the Swiss National Science Foundation (grant No. 21-57250.99) for financial support, and the Swiss Center for Scientific Computing in Manno, Switzerland, for a generous allocation of computer time.

Supporting Information Available: Comparison of bond lengths in experimental and calculated structures, and comparison of calculated bond orders (two tables). Graphical representation of the five highest occupied molecular orbitals in reactant and product compounds (two figures). This material is available free of charge via the Internet at http://pubs.acs.org.

References and Notes

(1) Mullen, G. E. D.; Went, M. J.; Wocadlo, S.; Powell, A. K.; Blower, P. J. *Angew. Chem., Int. Ed. Engl.* **1997**, *36*, 1205.
(2) Dilworth, J. R.; Parrott, S. J. *Chem. Soc. Rev.* **1998**, *27*, 43.
(3) Schoeneich, G.; Palmedo, H.; Heimbach, D.; Biersack, H. J.; Muller, S. C. *Onkologie* **1997**, *20*, 316.
(4) Prakash, S.; Went, M. J.; Blower, P. J. *Nucl. Med. Biol.* **1996**, *23*, 543.
(5) Mullen, G. E. D.; Blower, P. J.; Price, D. J.; Powell, A. K.; Howard, M. J.; Went, M. J. *Inorg. Chem.* **2000**, *39*, 4093.
(6) Cooper, S. R.; Rawle, S. C. *Struct. Bonding* **1990**, *72*, 1.
(7) Mullen, G. E. D.; Fässler, T. F.; Went, M. J.; Howland, K.; Stein, B.; Blower, P. J. *J. Chem. Soc., Dalton Trans.* **1999**, 3759.
(8) Magistrato, A.; Maurer, P.; Fässler, T.; Rothlisberger, U. *J. Phys. Chem. A* **2004**, *108*, 2008.
(9) Parrinello, M. *Solid State Commun.* **1997**, *102*, 107.
(10) Payne, M. C.; Teter, M. P.; Allan, D. C.; Arias, T. A.; Joannopoulos, J. D. *Rev. Mod. Phys.* **1992**, *64*, 1045.
(11) Remler, D. K.; Madden, P. A. *Mol. Phys.* **1990**, *70*, 921.
(12) Hutter, J.; Ballone, P.; Bernasconi, M.; Focher, P.; Fois, E.; Goedecker, S.; Parrinello, M.; Tuckerman, M. "*CPMD*"; Max-Planck Institut für Festkörperforschung, Stuttgart and IBM Research Laboratory: Zürich, 1998.
(13) Trouiller, N.; Martins, J. L. *Phys. Rev. B* **1991**, *43*, 1993.
(14) Kleinman, L.; Bylander, D. M. *Phys. Rev. Lett.* **1982**, *48*, 1425.
(15) Casteel, W. J.; Dixon, D. A.; LeBlond, N.; Mercier, H. P. A.; Schrobilgen, G. J. *Inorg. Chem.* **1998**, *37*, 340.
(16) Schäfer, L.; Seip, H. M. *Acta Chem. Scand.* **1967**, *21*, 737.
(17) Becke, A. D. *Phys. Rev. A* **1988**, *38*, 3098.
(18) Perdew, J. P. *Phys. Rev. B* **1986**, *33*, 8822.
(19) Lee, C.; Yang, W.; Parr, R. G. *Phys. Rev. B* **1988**, *37*, 785.
(20) Hockney, R. W. In *Methods in computational physics: advances in research and applications*; Alder, B.; Fernbach, S.; Rotenberg, M., Eds.; Academic Press: New York, 1970.
(21) Matondo, S. O. C.; Mountford, P.; Watkin, D. J.; Jones, D. J.; Cooper, S. R. *J. Chem. Soc., Chem. Commun.* **1995**, 161.
(22) White, D. J.; Kuppers, H. J.; Edwards, A. J.; Watkin, D. J.; Cooper, S. R. *Inorg. Chem.* **1992**, *31*, 5351.
(23) Rawle, S. C.; Sewell, T. J.; Cooper, S. R. *Inorg. Chem.* **1987**, *26*, 3769.
(24) Ziegler, T. In *Density-Functional Methods in Chemistry and Materials Science*; Springborg, M., Ed.; Wiley: New York, 1997.
(25) Magistrato, A.; VandeVondele, J.; Rothlisberger, U. *Inorg. Chem.* **2000**, *39*, 5553.
(26) MOLEKEL 4.0; Flükiger, P.; Lüthi, H. P.; Portmann, S.; Weber, J. Swiss Center for Scientific Computing, Manno (Switzerland), 2000.
(27) Bond orders were were calculated according to Mayer, I. *Chem. Phys. Lett.* **1983**, *97* (3), 270. To this end, the wave functions in the plane wave basis representation were projected onto an atom-centered minimal basis of atomic pseudo wave functions.
(28) This value (smaller than the dissociation limit) corresponds to a marginal barrier for dissociating ethene from the reactant. This barrier could also be an artifact arising from the choice of the constraint coordinate, or from the known difficulties of DFT in describing dissociation of molecules with an uneven number of electrons (see for example, Zhang, Y.; Yang, W. *J. Chem. Phys.* **1998**, *109*, 2604; Becke, A. D. *J. Chem. Phys.* **2003**, *119*, 2972).
(29) Calculations with atom-centered basis functions yield reaction energies that agree with the values in Table 2 within 2 kcal/mol, which confirms that the energetic differences indeed result from the correlation energy functionals, and not, for example, from the use of pseudopotentials. These calculations were carried out with the programm ADF2003.01 (te Velde, G. et al. *J. Comput. Chem.* **2001**, *22*, 931), using the builtin TZ2P basis set (triple-ζ + two polarization functions) and the ZORA relativistic approximation.